

Efficient fully nonlinear data assimilation for geophysical fluid dynamics

Article

Accepted Version

Van Leeuwen, P. J. and Ades, M. (2013) Efficient fully nonlinear data assimilation for geophysical fluid dynamics. *Computers & Geosciences*, 55. pp. 16-27. ISSN 0098-3004 doi: <https://doi.org/10.1016/j.cageo.2012.04.015> Available at <https://centaur.reading.ac.uk/35769/>

It is advisable to refer to the publisher's version if you intend to cite from the work. See [Guidance on citing](#).

To link to this article DOI: <http://dx.doi.org/10.1016/j.cageo.2012.04.015>

Publisher: Elsevier

All outputs in CentAUR are protected by Intellectual Property Rights law, including copyright law. Copyright and IPR is retained by the creators or other copyright holders. Terms and conditions for use of this material are defined in the [End User Agreement](#).

www.reading.ac.uk/centaur

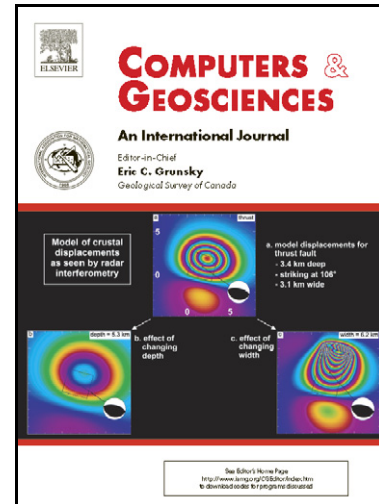
CentAUR

Central Archive at the University of Reading

Reading's research outputs online

Efficient fully nonlinear data assimilation for
geophysical fluid dynamics

Peter Jan van Leeuwen, Melanie Ades



PII: S0098-3004(12)00138-0
DOI: <http://dx.doi.org/10.1016/j.cageo.2012.04.015>
Reference: CAGEO2889

To appear in: *Computers & Geosciences*

Received date: 6 January 2012
Revised date: 16 April 2012
Accepted date: 19 April 2012

Cite this article as: Peter Jan van Leeuwen and Melanie Ades, Efficient fully nonlinear data assimilation for geophysical fluid dynamics, *Computers & Geosciences*, <http://dx.doi.org/10.1016/j.cageo.2012.04.015>

This is a PDF file of an unedited manuscript that has been accepted for publication. As a service to our customers we are providing this early version of the manuscript. The manuscript will undergo copyediting, typesetting, and review of the resulting galley proof before it is published in its final citable form. Please note that during the production process errors may be discovered which could affect the content, and all legal disclaimers that apply to the journal pertain.

1 Efficient fully nonlinear data assimilation for
2 geophysical fluid dynamics

3 Peter Jan van Leeuwen and Melanie Ades

4 *Data Assimilation Research Centre, Department of Meteorology, University of Reading, PO*
5 *Box 243, Reading, RG6 6BB, United Kingdom*

6 **Abstract**

7 A potential problem with Ensemble Kalman Filter is the implicit Gaussian as-
8 sumption at analysis times. Here we explore the performance of a recently pro-
9 posed fully nonlinear particle filter on a high-dimensional but simplified ocean
10 model, in which the Gaussian assumption is not made. The model simulates
11 the evolution of the vorticity field in time, described by the barotropic vorticity
12 equation, in a highly nonlinear flow regime. While common knowledge is that
13 particle filters are inefficient and need large numbers of model runs to avoid
14 degeneracy, the newly developed particle filter needs only of the order of 10-100
15 particles on large scale problems. The crucial new ingredient is that the proposal
16 density cannot only be used to ensure all particles end up in high-probability
17 regions of state space as defined by the observations, but also to ensure that
18 most of the particles have similar weights. Using identical twin experiments
19 we found that the ensemble mean follows the truth reliably, and the difference
20 from the truth is captured by the ensemble spread. A rank histogram is used to
21 show that the truth run is indistinguishable from any of the particles, showing
22 statistical consistency of the method.

23 *Key words:* Data Assimilation, Inverse Modeling, Particle Filter, Ensemble
24 Kalman Filter

25 1. Introduction

26 Numerical models for simulation and prediction of the evolution of systems in
27 the geosciences are becoming ever more complex. While relatively simple linear
28 balances tend to dominate the systems at large scales, with increasing resolution
29 more and more nonlinear processes are involved. Furthermore, with the coupling
30 of many physical, chemical and biological systems extremely complex behaviour
31 with highly nonlinear feedbacks has to be simulated.

32 To the extent that these flows are initial value problems our incomplete
33 knowledge of the exact initial conditions leads to incomplete knowledge of the
34 evolution of the system. This forces us to think in terms of uncertainty, which
35 can be described in probabilistic terms. The evolution equations for the related
36 probability densities have been known for decades (see e.g. Jazwinski, 1970).
37 If the system is Markovian, our present knowledge of the system in the form of
38 a probability density function evolves according to the Kolmogorov or Fokker-
39 Plank equation. This theory can be applied for small dimensional systems, but
40 the systems we study in the geosciences are not so.

41 When observations of the system are available, their information on the sys-
42 tem can be incorporated using Bayes Theorem, in which the prior probability
43 density function (pdf from now on), representing our prior knowledge, is mul-
44 tiplied by the likelihood, i.e. the probability density of the observations given
45 a specific model state. This then leads to the so-called posterior pdf, that de-
46 scribes our updated knowledge of the system. This process of updating the prior
47 pdf with observations is called *data assimilation*, and its goal is to determine
48 properties of this posterior pdf. It should be realised that this posterior pdf is
49 unlikely to be ever at our disposal in full because the size of the state space is
50 huge, typically 100 million for numerical weather prediction. We can only infer
51 statistical moments like mean, covariance, percentiles, and modes.

52 It is stressed here that the data-assimilation problem as specified above is a
53 multiplication problem and not an inverse problem: Bayes Theorem (see equa-
54 tion (1)) shows that one has to *multiply* the prior pdf with the likelihood to

55 obtain the posterior pdf. There is no inversion needed to obtain the poste-
56 rior. Also parameter estimation falls in this framework: the prior pdf of the
57 parameters is updated through multiplication with the likelihood to obtain the
58 posterior pdf of the parameters. Obviously, one needs the relation between the
59 parameters and the observations in the likelihood, and that typically involves
60 integrating a full numerical model, but that doesn't make the problem an in-
61 verse problem. The emphasis of this paper is on estimation of the pdf of the
62 model variables represented by a state vector, and not on that of parameters.

63 When the posterior pdf is unimodal or the majority of the posterior proba-
64 bility mass is concentrated around a mode of the posterior pdf it makes sense
65 to concentrate on the mode of the posterior pdf. The problem of finding the
66 mode is usually formulated as an inverse problem, i.e. a problem in which a
67 matrix has to be inverted, although there is no necessity to do so. Examples are
68 variational algorithms that try to find the mode by exploring the gradient of
69 the log of the posterior pdf. In the geosciences these methods are known as e.g.
70 gradient methods, 3DVar, 4DVar (Talagrand and Courtier, 1987), representer
71 method (Bennett, 1992), PSAS (Courtier, 1997), depending on details of the
72 solution method. The Ensemble Kalman filter (Evensen, 1994, Burgers et al.,
73 1998) is slightly different in that it tries to find the posterior mean (the least-
74 squares estimate, which is the mean by definition), but because of the linearity
75 assumptions in the Kalman filter it is assumed implicitly that the mean is close
76 to the mode. This has led to confusion that data assimilation is all about find-
77 ing this mode in the geophysical and the so-called inverse-problem communities,
78 and in some cases hampered progress to more nonlinear multimodal problems.

79 In this paper we propose solutions to highly nonlinear high-dimensional data-
80 assimilation problems. Our starting point is the particle filter (e.g. Gordon et al.,
81 1993), in which an ensemble of model runs is performed, representing our prior
82 knowledge of the system. Each ensemble member, or particle, is weighted with
83 its distance to observations when these become available. The distance norm
84 is determined by the value of the pdf of the observations given this particle,
85 so the likelihood of the observations given this particle. The weights are the

86 relative probabilistic weights of the particles, so e.g. the mean of the ensemble
87 now becomes a weighted mean in the posterior pdf.

88 It is well known that in systems with moderate dimensions, say of order
89 10 and higher, particle filters tend to be degenerate, meaning that the weights
90 vary too much. Typically after one or a few updates with observations the
91 relative weight of one particle is close to one, while that of all others is very
92 close to zero. This means that e.g. a weighted mean is in fact based on only one
93 particle, so all statistical information in the ensemble is lost. To prevent this
94 from happening several methods have been proposed, starting from resampling
95 (Gordon et al., 1993) to more complicated or approximating solutions (see e.g.
96 Doucet et al., 2001, and Van Leeuwen, 2009, for a review of applications in
97 the geosciences). None of the proposed methods is applicable to systems with
98 dimensions larger than say of order 100, without having to need millions of
99 particles, so millions of model integrations. As mentioned, our goal is perhaps
100 100 million dimensional systems, and this number keeps on increasing with the
101 size and speed of supercomputers.

102 In this paper we discuss a new particle filter methodology that is applicable
103 to systems of much higher dimension, and which up to the dimensions we tested
104 it on has perfect scaling, i.e. the number of particles is independent of the
105 dimension of the state vector. The secret is a proper use of the proposal den-
106 sity, that allows much more freedom than perhaps anticipated in earlier work.
107 Typically, the proposal density has been used to steer the particles to high-
108 probability areas as defined by the observations in state space, but when the
109 number of independent observations is large, the relative weights of the particles
110 will vary enormously, leading to degeneracy. Here we exploit the fact that the
111 proposal density can in addition be used to obtain similar relative weights for the
112 particles, thus avoiding degeneracy. The method is introduced in Van Leeuwen
113 (2010), and Van Leeuwen (2011) discussed applications to systems of up to 1000
114 dimensions using only about 20 particles. In this paper, the method is outlined
115 and its performance on a geophysical system with about 65,000 dimensions is
116 demonstrated.

117 The paper is organised as follows. The next section discusses Particle Fil-
 118 tering in general, followed by a section on the new method. It is highlighted
 119 why other particle filter formulations fail, and how the new method can be suc-
 120 cessful. Then the numerical model simulating the barotropic vorticity equation
 121 is described, followed by initial results when applying the new particle filter to
 122 that system. A concluding chapter closes the paper.

123 2. Particle filtering

The probability density function (pdf) of the state vector is represented, and approximated, by a discrete set of delta functions centred around a set of model states, called the particles. Using this representation of the prior pdf of the model in Bayes theorem

$$p(x|y) = \frac{p(y|x)p(x)}{\int p(y|x)p(x) dx} \quad (1)$$

where x is the state vector, and y is the observation vector, one finds:

$$p(x|y) = \sum_{i=1}^N w_i \delta(x - x_i) \quad (2)$$

in which the weights w_i are related to how close each particle is to the observations:

$$w_i = \frac{p(y|x_i)}{\sum_{j=1}^N p(y|x_j)} \quad (3)$$

The density $p(y|x_i)$ is the likelihood, i.e. the probability density of the observations given the model state x_i . It is related to the fact that we cannot make perfect observations, any observation comes with a measurement error, and hence this density is the pdf of the errors in the observations due to the measurement process. In the data-assimilation problem it is given, and often assumed to be Gaussian:

$$p(y|x_i) = A \exp \left[-\frac{1}{2} (y - H(x_i))^T R^{-1} (y - H(x_i)) \right] \quad (4)$$

124 in which $H(x_i)$ is the measurement operator, which projects the model state
 125 onto the observation space, R is the observation error covariance matrix, and A
 126 is a normalisation constant.

127 Unfortunately, weights vary wildly, and even when resampling is applied,
 128 only a few particles will have relatively high weight, so will have any statistical
 129 significance. This is called *filter degeneracy* and is a very serious problem in
 130 standard particle filtering (Snyder et al, 2008). Several methods have been
 131 proposed to solve this problem (see review for the geosciences by Van Leeuwen,
 132 2009), but none of these is directly applicable to large-dimensional geophysical
 133 problems.

134 To understand why this is the case, consider the following. Since the particles
 135 x_i are not the evolution of the true system, the distance in observation space
 136 between the observation y_j and the particle equivalent $H_j(x_i)$ will on average be
 137 similar to or larger than a typical observation error (from the Cauchy-Swartz
 138 inequality), so it can be expected that $(y_j - H_j(x_i))^T R_{jj}^{-1} (y_j - H_j(x_i))$ will
 139 typically be similar to or larger than 1 for each observation y_j . Assuming M
 140 independent observations, $(y - H(x_i))^T R^{-1} (y - H(x_i))$ is expected to be of
 141 order M or larger. So, to start with, the likelihood for each particle will be
 142 fairly small.

143 However, the particle filter works with relative weights, so we need to ad-
 144 dress the variation of the likelihood with the particles. Let us assume that the
 145 particles are drawn from a Gaussian with covariance B centred around the true
 146 state. Clearly, the larger B , the larger the variation in the weights of the par-
 147 ticles. Let us now assume, to illustrate the argument, that HBH^T is of similar
 148 magnitude as R . In that case, the argument of the exponent in the likelihood
 149 is a χ -squared variable with M degrees of freedom. Such a variable has mean
 150 M , and standard deviation $\sqrt{2M}$. This means that the relative weights of the
 151 particles differ by a factor $\exp \sqrt{2M}$. Assuming a moderate 50 independent ob-
 152 servations, the weights will vary by a factor $\exp(50) \approx 5.0 \cdot 10^{21}$, so the particle
 153 filter will be degenerate when the number of independent observations grows,
 154 and serious improvement is needed.

155 **3. The new method**

The new method that will be explored consists of two ingredients. The first ingredient is that the particles are steered towards the future observations by choosing a specific form of model forcing that tends to pull the model towards the observations. This is an old idea in particle filtering, and has been explored in the Lorenz 1963 and 1996 models in Van Leeuwen (2010, 2011). Assume the model equation to be written as

$$x^n = f(x^{n-1}) + \beta^n \quad (5)$$

in which $f(\cdot)$ denotes the deterministic part of the model and β^n is the stochastic part, and n is the time index. Instead of using this, the model equation is modified to:

$$x^n = f(x^{n-1}) + \hat{\beta}^n + K(y^m - H(x^{n-1})) \quad (6)$$

156 in which $\hat{\beta}^n$ is random forcing which might have different characteristics from
 157 the original random forcing, and y^m denotes future observations at time $m > n$.
 158 The main difference with the original model equation is the relaxation term that
 159 tends to pull the particle to the future observations y^m with a strength given
 160 by matrix K . This relaxation matrix will depend on the application, and an
 161 example is given below. This looks like cheating in the sense that the model
 162 forcing is not chosen from the probability density of the model error, but as
 163 something that we like better. Also, the different particles will have different
 164 strength of the 'pulling' term dependent on how far they are from the future
 165 observations, so we seem to lose control over the statistical meaning of each
 166 particle. However, this different forcing can be compensated for exactly by
 167 changing the relative weights of the particles.

In particle filter jargon, we have implemented a proposal transition density instead of using the original transition density. The original transition density is denoted as $p(x^n|x^{n-1})$ specifying how probable state x^n is given state x^{n-1} at the previous time step. For the original model equation (5) this density is

given by the pdf of β^n . If the β^n are Gaussian distributed as $N(0, Q)$, we find:

$$p(x^n|x^{n-1}) = N(f(x^{n-1}), Q) \quad (7)$$

The proposal transition density can be written as, assuming a Gaussian distribution for the $\hat{\beta}^n$ with covariance \hat{Q} :

$$q(x^n|x^{n-1}, y^m) = N(f(x^{n-1}) + K(y^m - H(x^{n-1})), \hat{Q}) \quad (8)$$

168 Also \hat{Q} can be problem dependent. In the example discussed below we choose it
 169 equal to Q . Note that the proposal transition density does depend on the future
 170 observations. Furthermore, the relaxation term is part of the deterministic
 171 proposal model, since the observations are given.

The question now is how the weights are affected when we arrive at the observations at time m . To this end, let us write the prior pdf at time m as:

$$\begin{aligned} p(x^m) &= \int p(x^m, x^{m-1}, \dots, x^0) dx^{m-1} \dots dx^0 \\ &= \int p(x^m|x^{m-1}) \dots p(x^1|x^0) p(x^0) dx^{0:m-1} \end{aligned} \quad (9)$$

in which we exploited the Markovian property of the model, and introduced the shorthand notation $dx^{n-1} \dots dx^0 = dx^{0:n-1}$. Furthermore, the previous set of observations was present at time 0 in this notation. The integrand can be multiplied and divided by the proposal transition densities to find:

$$p(x^m) = \int \frac{p(x^m|x^{m-1})}{q(x^m|x^{m-1}, y^m)} \dots \frac{p(x^1|x^0)}{q(x^1|x^0, y^m)} q(x^m|x^{m-1}, y^m) \dots q(x^1|x^0, y^m) p(x^0) dx^{0:n-1} \quad (10)$$

In the original model we draw random samples from $p(x^0)$ and from each of the $p(x^i|x^{i-1})$ as indicated above. Using the proposed model we draw samples from $p(x^0)$ and from the proposal transition densities $q(x^i|x^{i-1}, y^m)$. Doing the latter, realising that this creates delta functions for times 0 to $n-1$, we can perform the integrations and find for the prior at time m :

$$p(x^m) = \sum_{i=1}^N \hat{w}_i \delta(x - x_i) \quad (11)$$

in which the weights are given as:

$$\hat{w}_i = \frac{p(x_i^m | x_i^{m-1})}{q(x_i^m | x_i^{m-1}, y^m)} \cdots \frac{p(x_i^1 | x_i^0)}{q(x_i^1 | x_i^0, y^m)} \quad (12)$$

172 So where we had equally weighted particles in the standard particle filter for
 173 the prior, we now have weighted particles. These weights are related to the fact
 174 that we changed the model equations. They specify how probable the move
 175 from x^n to x^{n-1} is in the original model, normalised by that probability in the
 176 modified model.

Finally, to find the full posterior weights we use Bayes theorem to include the likelihood, leading to

$$w_i \propto p(y^m | x_i^m) \frac{p(x_i^m | x_i^{m-1})}{q(x_i^m | x_i^{m-1}, y^m)} \cdots \frac{p(x_i^1 | x_i^0)}{q(x_i^1 | x_i^0, y^m)} \quad (13)$$

177 Making sure that all particles end up relatively close to the observations still
 178 does not avoid wildly varying weights in large-dimensional systems. Clearly,
 179 ending up close to the observations reduces the variance in the likelihood weights,
 180 but the variance in the weights related to the proposal density are nonzero, and
 181 can be substantial.

182 The second new ingredient is that we ensure that all posterior weights are of
 183 equivalent size. This is achieved in two stages: first, use the scheme mentioned
 184 above for all time steps up to time $n - 1$ and perform a deterministic time step
 185 with each particle that ensures that most of the particles have equal weight; and
 186 secondly, add a very small random perturbation to ensure that Bayes theorem
 187 is satisfied. There are many ways to accomplish both stages.

Let us assume that the observation errors and the errors in the model equations are Gaussian distributed. The weights can be written as:

$$w_i \propto p(y^m | x_i^m) \frac{p(x_i^m | x_i^{m-1})}{q(x_i^m | x_i^{m-1}, y^m)} w_i^{rest} \quad (14)$$

leaving the last time step open. w_i^{rest} contains the weights from all time steps up to time $n - 1$, which are now given (we have done all these steps). Ignoring the proposal transition density part for the moment, making the weight of each

particle equal to $\exp(-C)$, say, leads to the following quadratic equation for particle x_i at time m :

$$\frac{1}{2}(x^m - f(x_i^m))^T Q^{-1}(x^m - f(x_i^m)) + \frac{1}{2}(y - Hx_i^m)^T R^{-1}(y - Hx_i^m) - \log(w_i^{rest}) = C \quad (15)$$

188 Now any quadratic form has a minimum, and depending on the value for C this
 189 equations has two, one, or zero real roots for a one dimensional system. Zero
 190 roots means that the particle is unable to reach this specified weight $\exp(-C)$;
 191 the w_i^{rest} factor for such a particle is too low. Clearly, we don't want the weight
 192 of each particle to be the same as the worst particle. We have chosen here a
 193 weight C such that 80% can reach it, and the other 20% will be ignored for now.
 194 They will re-enter the ensemble via the resampling step later on.

Once C is chosen, an infinite number of solutions exist if the dimension of the system is larger than 1. A simple choice is to enforce

$$x_i^m = f(x_i^{m-1}) + \alpha_i M (y^m - H(f(x_i^{m-1}))) \quad (16)$$

in which $M = QH^T(HQH^T + R)^{-1}$, Q is the error covariance of the model errors, and R is the error covariance of the observations. α_i is a scalar that is determined from equation (15), and we obtain for each α_i , (see Van Leeuwen, 2010, 2011)]:

$$\alpha_i = 1 - \sqrt{1 - b_i/a_i} \quad (17)$$

195 in which $a_i = 0.5x_i^T R^{-1} H K z$ and $b_i = 0.5x_i^T R^{-1} x_i - C - \log w_i^{rest}$. Here
 196 $z = y^m - H(f(x_i^{m-1}))$, C is the chosen weight level, and w_i^{rest} denotes the
 197 relative weights of each particle i up to this time step, related to the proposal
 198 density explained above.

199 Note that the last time step so far is a purely deterministic step: we have
 200 chosen C , and directly calculated x_i^m . Of course, this last step towards the
 201 observations cannot be fully deterministic, as can be seen from Eq. (13). A
 202 deterministic proposal would mean that the proposal transition density q can
 203 be zero while the target transition density p is non zero, leading to division by

204 zero: a deterministic move the transition density is a delta function. In the
 205 example presented below the proposal transition density was chosen to be a
 206 Gaussian. Since the weights have q in the denominator a draw from the tail of
 207 a Gaussian could lead to a very high weight for a particle that is perturbed by a
 208 relatively large amount, resulting in the opposite of the intended outcome. We
 209 didn't encounter this problem in this experiment.

To avoid this potential problem q could be chosen in the last step before the observations as a mixture density

$$q(x^m|x') = (1 - \gamma)U(-a, a) + \gamma N(0, a^2) \quad (18)$$

210 in which x' is the particle after the deterministic step outlined above. A draw
 211 from this density would be performed as follows. First, we determine from which
 212 density U , or N , we will draw the stochastic perturbation, e.g. by drawing u
 213 from a uniform density $U[0, 1]$ and if $u < \gamma$ we draw from the normal density
 214 $N(0, a^2)$, and we draw from the uniform density $U(-a, a)$ otherwise. By choos-
 215 ing γ very small we most likely draw from the uniform density $U(-a, a)$. For
 216 small a we can completely control the size of the stochastic perturbation to the
 217 state vector. If by chance we have to choose from $N(0, a^2)$ we most likely draw
 218 from near the peak of this Gaussian. It is very unlikely to draw from the Gaus-
 219 sian and at the same time draw from the tail of that Gaussian. It is mentioned
 220 that γ can be made dependent on the number of particles to control the number
 221 of times we actually draw from the Gaussian, and keep that number small.

222 4. The barotropic vorticity equation and statistical set up

The barotropic vorticity equation describes how the vorticity field ζ changes with time through advection of the vorticity field by the velocity field:

$$\frac{\partial q}{\partial t} + u \frac{\partial q}{\partial x} + v \frac{\partial q}{\partial y} = \beta \quad (19)$$

in which u the eastward and v the northward velocity, and in which we included a random forcing β . The vorticity field is related to the velocity field as

$$\zeta = \frac{\partial v}{\partial x} - \frac{\partial u}{\partial y} = 0 \quad (20)$$

Because the divergence of the horizontal velocity field is zero:

$$\frac{\partial u}{\partial x} + \frac{\partial v}{\partial y} = 0 \quad (21)$$

a streamfunction can be defined as

$$u = -\frac{\partial \psi}{\partial y} \quad v = \frac{\partial \psi}{\partial x} \quad (22)$$

Combining this with the evolution equation for the vorticity field leads to the following set of equations that have to be solved at every time step:

$$\begin{aligned} \frac{\partial q}{\partial t} - \frac{\partial \psi}{\partial y} \frac{\partial q}{\partial x} + \frac{\partial \psi}{\partial x} \frac{\partial q}{\partial y} &= \beta \\ q &= \frac{\partial^2 \psi}{\partial x^2} + \frac{\partial^2 \psi}{\partial y^2} \end{aligned} \quad (23)$$

223 This set of equations is solved on a double periodic domain of 256 by 256 grid
 224 points and grid spacing $\Delta x = \Delta y = 1/256$, leading to a state dimension of
 225 close to 65,000. At each time step the vorticity field is updated using a semi-
 226 Lagrangian scheme with time step $\Delta t = 0.04$, followed by an update of the
 227 streamfunction via an inversion of the second equation using FFT's.

228 The stochastic term is chosen from a multivariate Gaussian with mean zero,
 229 variance 0.01, and a Gaussian spatial correlation with decorrelation lengthscale
 230 4 gridpoints. It is integrated using a simple Euler scheme. Because we are not
 231 interested in the specific stochastic evolution, but in the overall properties of the
 232 stochastic equation, the accuracy is $O(\Delta t)$. The initial condition was a random
 233 vorticity field with nondimensional amplitude 1 and spatial decorrelation length
 234 of 10 grid points. This initial condition results in highly nonlinear turbulent
 235 flow structures. Without the random forcing, the evolution of the system would
 236 follow that of 2-D turbulence, cascading energy to the largest scales. However,
 237 the random forcing keeps on injecting energy at smaller scales, so the flow
 238 remains fully turbulent throughout the whole data assimilation experiment. The
 239 whole experiment lasted 600 time steps.

240 The vorticity field was observed every 50 time steps on every gridpoint, giv-
 241 ing about 65,000 observations every time step. The observations were obtained

242 from a truth run and independent random measurement noise with standard
243 deviation 0.05 was added to each observation. This should be compared to the
244 typical nondimensional vorticity values of about 1. We determined the decor-
245 relation timescale τ of the system by averaging the correlation time series at
246 several points in the field, and taking τ as the time scale at which the correlation
247 was $1/e$. We found a decorrelation time scale of this system of about 26 time
248 steps. Since we observe the system every 50 time steps this is an extremely hard
249 nonlinear data assimilation problem.

250 Only 24 particles were used to track the posterior pdf. Because we observe
251 the full state vector we chose K in the relaxation term as a scalar with maximum
252 value $K = 0.1$. (In general, when only part of the state vector is observed, or
253 when H is a nonlinear function, K will be a matrix.) The random forcing
254 covariance \hat{Q} was the same as in the original model Q . This value for K is equal
255 to the standard deviation of the model errors, chosen such that the relaxation
256 term will be of that order of magnitude. Furthermore, K was chosen to vary
257 linearly from zero to its maximum value between observation times. This allows
258 the ensemble to spread out due to the random forcing initially, and pulling
259 harder and harder towards the new observation the closer the system comes to
260 the new observation time. No tuning has been applied in this example of the
261 new particle filter, the reasonable values used for the parameters in the scheme
262 applied to the Lorenz 1993 and 1996 systems (see Van Leeuwen, 2010,2011) have
263 been implemented directly. More detailed experiments in which the sensitivity
264 of the results to these specific choices for K will be described in another paper
265 in preparation.

266 5. Results

267 Here a few initial results using the new particle filter with equivalent weights
268 are shown. Figure 1 shows the vorticity field at time 50, and figure 2 the mean of
269 the particles at that time. The two field are almost identical to the eye, showing
270 that the new method is able to track the truth in this highly nonlinear regime.

271 Figure 3 shows the vorticity field at time 600, and its particle filter counterpart
272 is shown in figure 4. Again the close tracking is very encouraging.

273 Figure 5 shows the absolute value of the difference between the ensemble
274 mean and the truth run at time 50. This can be compared to the standard
275 deviation in the ensemble in figure 6. Figures 7 and 8 show the same, but now
276 after 600 time steps. Although the spread around the truth is underestimated
277 at several locations, it is over estimated elsewhere, and the averages over the
278 fields are almost equal. Given the statistical nature of these estimates, this is
279 satisfactory.

280 A check on the workings of the equivalent weights scheme is to visualise the
281 weights before resampling. Figure 9 shows that the weights are distributed as
282 they should: they display small variance around the equal weight value $1/20$
283 for the 80% of the 24 particles. Note that the particles with zero weight had
284 too small weight to be included in the equivalent weight scheme, and will be
285 resampled from the rest. Because the weights vary so little the weights can
286 be used back in time, generating a smoother solution for this high-dimensional
287 problem with only 24 particles. The results presented here refer to the filter
288 solution only.

289 One of the questions one could ask is if these results could have been obtained
290 with one of the standard scheme's used in meteorology or oceanography, like
291 4DVar or variants of the EnKF. When concentrating on the mean this might be
292 so, but clearly the structure of the full pdf cannot be reconstructed with these
293 methods. An example is depicted in figure 10, which shows the posterior pdf
294 for the vorticity value at a certain point after 600 time steps. The non-Gaussian
295 structure, hinting at bimodality, cannot be captured by any of these traditional
296 methods.

297 Variational methods like 4DVar typically provide no error estimate because
298 that is too expensive for large-dimensional problems like encountered in e.g.
299 numerical weather prediction. From a scientific point of view this is not satis-
300 factory. Furthermore, in a situation like depicted in figure 10 the usefulness of
301 just the modal value would be limited, and also an error estimate based on the

302 Hessian, so the local curvature, has limited significance. Finally, given that the
303 observation times are about two decorrelation time scales apart, 4DVar might
304 struggle to convergence, but that is not tested here.

305 Ensemble Kalman filter methods do assume Gaussian prior and posterior
306 densities. It might be possible by tuning inflation factors and localisation func-
307 tions to obtain a proper evolution of the ensemble mean, comparable with the
308 true evolution of the system. The ensemble generated with an EnKF might
309 show bimodal structures, but it is unclear if these are real since the update does
310 assume Gaussian pdf's, leading to a posterior pdf that does not have the correct
311 posterior mean and covariance (under the Gaussian assumption). The actual
312 positions of the ensemble members differ in the different variants of the ensem-
313 ble Kalman filter and have no direct statistical meaning. Furthermore, it is
314 unclear if the ensemble covariance would have any real scientific meaning for
315 these highly non-Gaussian pdf's. The ensemble spread is perhaps more used
316 for tuning the system to ensure the correct evolution of the mean via inflation
317 and localisation, than representing actual covariances in these highly nonlinear
318 systems.

319 It is stressed here that no tuning has been applied in this example of the
320 new particle filter, the reasonable values used for the parameters in the scheme
321 applied to the Lorenz 1993 and 1996 systems (see Van Leeuwen, 2010, 2011)
322 have been implemented directly.

323 An important issue is the quality of the scheme to infer the full posterior pdf.
324 We have seen that the mean is close to the truth, but that could be due to e.g.
325 extreme relaxation, so that all particles are very close to the observations, and
326 so close to the truth in this high dimensional system. To investigate the quality
327 of the ensemble we calculated a rank histogram using the ensemble values at
328 every 50th time step and at every 4th grid point in each row and column of the
329 field, assuming they were close to independent. For each time instance we rank
330 the value of the truth in each gridpoint in the ensemble values at that gridpoint.
331 This is done through ranking the values for the ensemble members from low to
332 high, and determining where the truth lies in this ranking. The rank histogram

333 is constructed by adding a value of 1 to that bin in which the truth falls, e.g. bin
334 4 is increased by 1 if the truth ranks between ensemble member 3 and 4. This
335 is repeated for each gridpoint as mentioned above, and for each time instance,
336 generating one rank histogram. The result is depicted in figure 11.

337 The second way to generate a rank histogram is to rank the observations in
338 the measured ensemble members perturbed by the normal measurement error.
339 This is the method of choice when the truth is not available, as in any real
340 situation. Figure 11 shows the ranking of the truth, but both methods give
341 similar results.

342 In the ideal case any of the particles could act as the truth, resulting in a
343 uniform histogram. A low bias of the particles would yield a histogram in which
344 the truth is biased to the higher rankings, so a histogram with higher bins to
345 the right, and vice versa. An under dispersive ensemble will give rise to a truth
346 value that is either lower or higher than the typical ensemble, resulting in a
347 U-shaped histogram. Finally, an over dispersive ensemble leads to a histogram
348 with a hump in the middle. Although the present histogram in figure 11 is
349 not uniform, it is close to it given the statistical noise. One could do a proper
350 confidence interval test, but that is not attempted here. It is remarkable to
351 see how flat the histogram is, realising the high dimension of the system, the
352 long interval between observations, and the fact that we only use 24 particles.
353 The hump in the middle of the histogram might indicate an over dispersive
354 ensemble, but the peaks at the end of the interval tend to show the opposite,
355 an under dispersive ensemble. Or perhaps we see an over dispersive ensemble
356 with biases in both directions. This little discussion shows that weakness of
357 the histogram, it can be nearly flat for several reasons, not all of them positive.
358 But, notwithstanding that, the results are encouraging.

359 The results so far are encouraging and a much more detailed analysis of the
360 present results, looking e.g. more closely at the posterior pdf's, the sensitivity
361 to the observation uncertainty, and the spatial and temporal frequency of the
362 observations. This will be reported on in a future paper.

363 6. Conclusions and discussion

364 The effectiveness of a new particle filter that exploits the proposal density
365 and allows small ensemble sizes has been demonstrated on the highly nonlin-
366 ear 65,000 dimensional barotropic vorticity equation that simulates ocean eddy
367 processes. It was shown using identical twin experiments that the ensemble
368 mean closely follows the truth, and that the ensemble spread is a good measure
369 of the difference between the two. The nonlinear character of the problem is
370 highlighted by studying the posterior pdf's, which often tend to show bimodal
371 behaviour. Finally, a rank histogram for the whole experiment was shown to be
372 close to uniform, indicating that the statistics of the ensemble is sound.

373 The advantage of this method is the enormous freedom in the two steps that
374 make up the new method. The first adds terms to the model equations that
375 force the model towards the future observations. The simple additive terms
376 allow easy implementation in any simulation code for atmosphere or ocean, or
377 more generally any computer code that simulates a Markov process. But also
378 more sophisticated proposals can be used, like methods that optimise paths on
379 each particle, e.g. a weak-constraint 4DVar solution on each particle. Note
380 that the 4DVar would be special in the sense that the initial condition of the
381 4DVar is fixed, the particle position at time zero, but a model error term has to
382 be included. Furthermore, since a 4DVar is a deterministic solution a random
383 perturbation has to be added to each time step after the full 4DVar solution has
384 been obtained.

385 The second crucial step allows the weights to be almost equal. Without
386 this step the particle filter would still be degenerate with a large number of
387 independent observations in the present settings. Also here much freedom exists
388 in how this term is implemented. We replaced the search for the intersection
389 of a hyperplane and the pdf in the 65,000 dimensional space by a simple line
390 search, but many other possibilities can be explored. There is an interesting
391 connection with new developments in rare event simulation using Monte-Carlo
392 methods. Also there good proposal densities are essential, and advances have

393 been made that allow simulation with minimal Monte-Carlo statistical errors
394 (see e.g. Vanden Eijnden and Weare, 2012). These links will be pursued in
395 future work.

396 One of the main questions is why this particle filter works in this high-
397 dimensional system with only 24 particles. The reason is not entirely clear
398 yet, but is most likely related to the following. First, one has to realise that
399 there is no inherent problem related to the size of the space spanned by a small
400 number of the particles with a high number of independent observations. (This
401 would be the case for an ensemble Kalman filter.) The clearest examples are
402 variational methods like 4DVar that are able to absorb all observations in a
403 single model run. In the present implementation of the particle filter we do
404 not run a complete 4DVar on each particle but a very crude approximation to
405 that through the relaxation term. (One could run a 4DVar on each particle,
406 as mentioned above, which is what the implicit particle filter of Chorin and
407 Tu (2009) does, but that would be much more expensive, although probably
408 better.) This, however is not enough to avoid filter divergence of the particle
409 filter, i.e. the fact that the likelihood and proposal weights vary too much, with
410 one particle getting a weight close to one, and the others all weights close to zero,
411 when the number of independent observations is large. For that a scheme like
412 the equivalent-weights step is needed to allow for the majority of the particles
413 to have very similar weights, thus avoiding degeneracy. The actual dimension
414 of the manifold on which the dynamics happens will be (much) smaller than
415 the 65,000. The barotropic vorticity dynamics exhibits spatial and temporal
416 coherency in which the smaller-scale motions tend to be slaved to the larger
417 scales. (However, it should be realised that the small-scale random forcing does
418 destroy this coupling to some extent.) It should be realised that of interest is
419 the dimension of the dynamics given the observations, which will be different
420 from that of the dynamical manifold of a free run. Exploring this fact is a very
421 exciting research direction in which the data assimilation community and the
422 dynamical systems community will have to work closely together. It will be
423 clear, however that the dimension of this manifold will be much higher than 24.

424 Some variant of the EnKF could be used as proposal density for the particle
425 filter, allowing e.g. for localisation, which is not straightforward in particle
426 filtering (see e.g. Van Leeuwen, 2009, Papadakis et al, 2010, Prakash et al,
427 2011). This might allow us to ignore the relaxation scheme at each time step.
428 The localised EnKF scheme could then be followed by the equivalent weights
429 scheme. This is one direction of further research.

430 One of the main advantages of this particle filter scheme is that no reference
431 is made to the covariance of the model state. It is well known that 4DVar
432 stands or falls with the quality of the covariance of the initial state, the so-
433 called B matrix. An enormous research effort has been spent, and is still spent
434 on improving this B matrix. Also Ensemble Kalman Filters rely on the accuracy
435 of the ensemble covariance matrix. This is why so much effort has gone into,
436 and is still going into better inflation and localisation schemes. All these issues
437 play no role in particle filtering.

438 It is well realised in the geosciences community that errors in the model
439 equations have to be included in the data-assimilation schemes. However, a
440 proper statistical description of these errors is hard to come by. Even if it is
441 assumed that the errors are Gaussian distributed, the mean, related to a model
442 bias, and its covariance need to be specified, which is not easy. But that doesn't
443 mean we should not go forward, especially when we realise that this will be the
444 proper way to model improvement. As soon as an estimate of the statistical
445 properties of the model errors is obtained, implementation in ensemble data
446 assimilation methods like EnKf and particle filters is relatively easy because
447 random realisations for these error estimates can be added directly to each
448 ensemble member (and similar for multiplicative errors). Much more research
449 is needed to come up with efficient implementations in variational methods.
450 So, particle filters like the one explored here force us to consider where we are
451 weakest: the errors in the model equations, and these particle filters are not
452 distracted by problems in covariance structures in the model states themselves.

453 Although the results presented here might be promising, much more research
454 is needed before questions on suitability for e.g. numerical weather forecasting

455 can be answered. For example, we observed the full state vector at observation
456 times, which is never the case for any real application from the geosciences.
457 We are working hard on partially observed systems now. On the other hand,
458 we observed the system at twice the decorrelation time scale, which makes the
459 problem extremely hard since the information from previous observations is lost
460 to a very large extent, showing the robustness of the method.

461 Another critical issue is to what extent the method pulls the system out
462 of quasi balanced states. In numerical weather prediction tremendous progress
463 was made when models were forced to stay close to balanced states, greatly
464 suppressing artificial gravity waves that ruined the forecasts. It should be re-
465 alised that as soon as we accept a statistical description of model errors model
466 balances will be perturbed. So the question is if and how the proposal den-
467 sity will perturb the model balances more than just the random forcing. By
468 keeping the stochastic part of the proposal density of similar magnitude as the
469 original transition density that part should not add extra perturbations. The
470 deterministic relaxation term can grow quite large, but if that becomes problem-
471 atic we can restrict its size to some maximum value without problem. Another
472 option is to project the relaxation terms to some sort of slow manifold, as is
473 done in high-resolution numerical weather prediction ensemble Kalman filter
474 applications. However, when the dynamics is strongly nonlinear it is unclear
475 what the actual balances are. Finally, the essential equivalent weights step can
476 be large too. Also here we could limit the size of the deterministic move, but
477 this might destroy the possibility for majority of the weights to be equivalent.
478 Also, projection on a slow manifold might help here too, with the same caveat
479 as above. More research into these aspects are needed, and will no doubt be
480 problem dependent.

481 **Acknowledgements**

482 We thank the National Centre for Earth Observation (NCEO) and the Na-
483 tional Environmental Research Council (NERC) for support via grants. Also

484 two anonymous reviewers are thanked for critical comments that improved the
485 paper substantially.

486 REFERENCES

- 487 Bennett, A., 1992, *Inverse Methods in Physical Oceanography*, Cambridge Uni-
488 versity Press, Cambridge.
- 489
- 490 Burgers, G., Van Leeuwen, P.J., and Evensen, G., 1998, Analysis Scheme in the
491 Ensemble Kalman Filter, *Monthly Weather Review*, 126, 1719-1724.
- 492
- 493 Chorin, A.J., and X. Tu, 2009, Implicit sampling for particle filters, *PNAS*, 106,
494 17249-17254.
- 495
- 496 Courtier, P., 1997, Dual formulation of four-dimensional variational assimila-
497 tion, *Quarterly Journal of the Royal Meteorological Society*, 123(B), 2449-2461.
- 498
- 499 Doucet, A., De Freitas, N., and Gordon, N., 2001, *Sequential Monte-Carlo meth-*
500 *ods in practice*, Springer, Berlin.
- 501
- 502 Evensen, G., 1994, Sequential data assimilation with a nonlinear quasi-geostrophic
503 model using Monte-Carlo methods to forecast error statistics, *Journal of Geo-*
504 *physical Research*, 99, 10143-10162.
- 505
- 506 Gordon, N.J., D.J. Salmond, and A.F.M. Smith., 1993, Novel approach to
507 nonlinear/non-Gaussian Bayesian state estimation, *IEEE Proceedings-F*, 140,
508 107-113.
- 509
- 510 Jazwinski, A.H., 1970, *Stochastic processes and filtering theory*, Academic Press,
511 376p.
- 512 Papadakis, N., E.Memin, A. Cuzol, and N.Gengembre, 2010, Data assimilation
513 with the weighted ensemble Kalman filter, *Tellus*, 62, 673-697.

- 514 Prakask J., S.C.Patwardhan, and S.L.Shah, 2011, On the choice of importance
515 distributions for unconstrained and constrained state estimation using particle
516 filters, *J. Process Control*, 21, 3-16.
517
- 518 Snyder, C., T. Bengtsson, P. Bickel, and J. Anderson, 2008, Obstacles to high-
519 dimensional particle filtering, *Monthly Weather Review*, 136, 4629-4640.
520
- 521 Talagrand, O., and P. Courtier, 1987, Variational assimilation of meteorological
522 observations with the adjoint vorticity equation. I: Theory, *Quarterly Journal*
523 *of the Royal Meteorological Society*, 113, 1311-1328.
524
- 525 Vanden Eijnden E. and J. Weare, 2012, Rare event simulation with vanishing
526 error for small noise diffusions, *Communications Pure Applied Math.*, in press.
- 527 Van Leeuwen, P.J., 2009, Particle Filtering in Geosciences, *Monthly Weather*
528 *Review*, 137, 4089-4114.
529
- 530 Van Leeuwen, P.J., 2010, Nonlinear Data Assimilation in geosciences: an ex-
531 tremely efficient particle filter, *Quarterly Journal of the Royal Meteorological*
532 *Society.*, 136, 1991-1996.
533
- 534 Van Leeuwen, P.J. 2011, Efficient non-linear Data Assimilation in Geophysical
535 *Fluid Dynamics, Computers and Fluids*, doi:10.1016/j.compfluid.2010.11.011.

536 **List of Figures**

- 537 1 Snap shot of the vorticity field of the truth at time 50. Note the
538 highly chaotic state of the field. 24
- 539 2 Snap shot of the vorticity field of the mean of the particle filter
540 mean at time 50. Compare with figure 1 and note the close to
541 perfect tracking. 25
- 542 3 Snap shot of the vorticity field of the truth at time 600. Note
543 again the highly chaotic state of the field. 26

544	4	Snap shot of the vorticity field of the mean of the particle filter	
545		mean at time 600. Compare with figure 3 and note the close to	
546		perfect tracking.	27
547	5	Snap shot of the absolute value of the mean-truth misfit at time	
548		50. Note the highly irregularity of the field, reflecting the statis-	
549		tical nature of the estimate.	28
550	6	Snap shot of the absolute value of the standard deviation in the	
551		ensemble at time 50 for comparison with figure 5. The ensemble	
552		underestimates the spread at several locations, but averaged over	
553		the field it is slightly higher, 0.074 versus 0.056.	29
554	7	Snap shot of the absolute value of the mean-truth misfit at time	
555		600.	30
556	8	Snap shot of the absolute value of the standard deviation in the	
557		ensemble at time 600 for comparison with figure 7	31
558	9	Weights distribution of the particles before resampling. All weights	
559		cluster around 0.05, which is close to $1/24$ for uniform weights	
560		(using 24 particles). The 5 particles with weights zero will be re-	
561		sampled. Note that the other particles form the smoother estimate. 32	
562	10	Estimate of the posterior pdf of the vorticity value at point (200,200)	
563		after 600 time steps. The bimodal structure shows that vari-	
564		ational methods that look for the mode of this pdf have little	
565		meaning, and also methods based on the EnKF will not be able	
566		to represent this structure accurately.	33
567	11	Rank histogram of how the truth ranks in the ensemble. The	
568		nearly uniform distribution shows that each particle could act as	
569		the truth, suggesting the ensemble is of good quality. (But see	
570		discussion in text.)	34

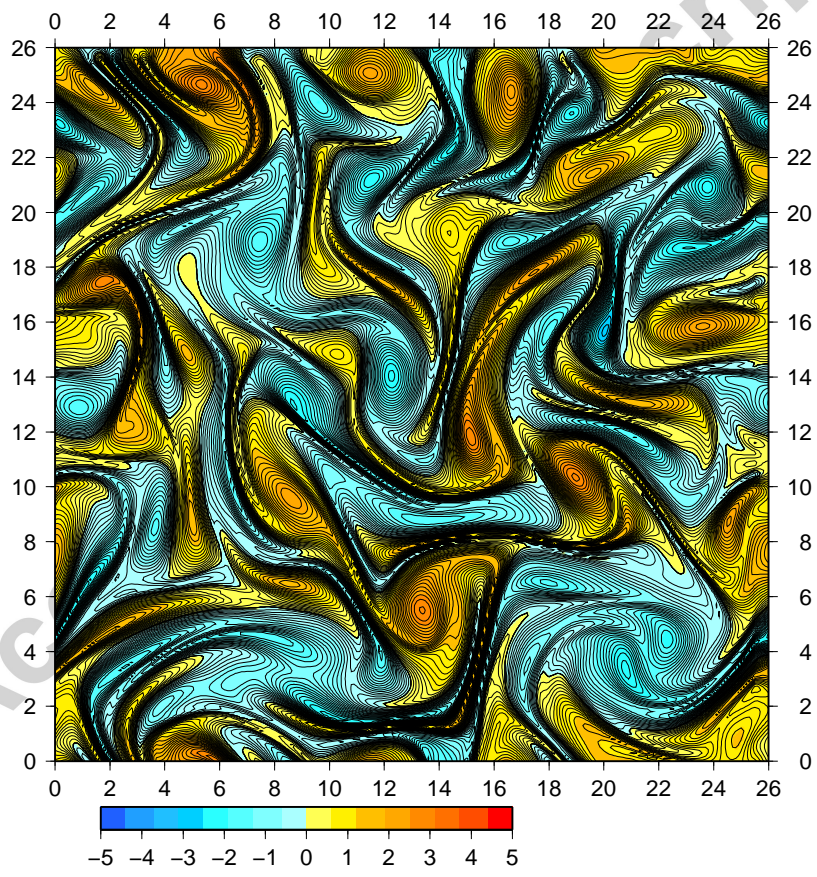


Figure 1: Snap shot of the vorticity field of the truth at time 50. Note the highly chaotic state of the field.

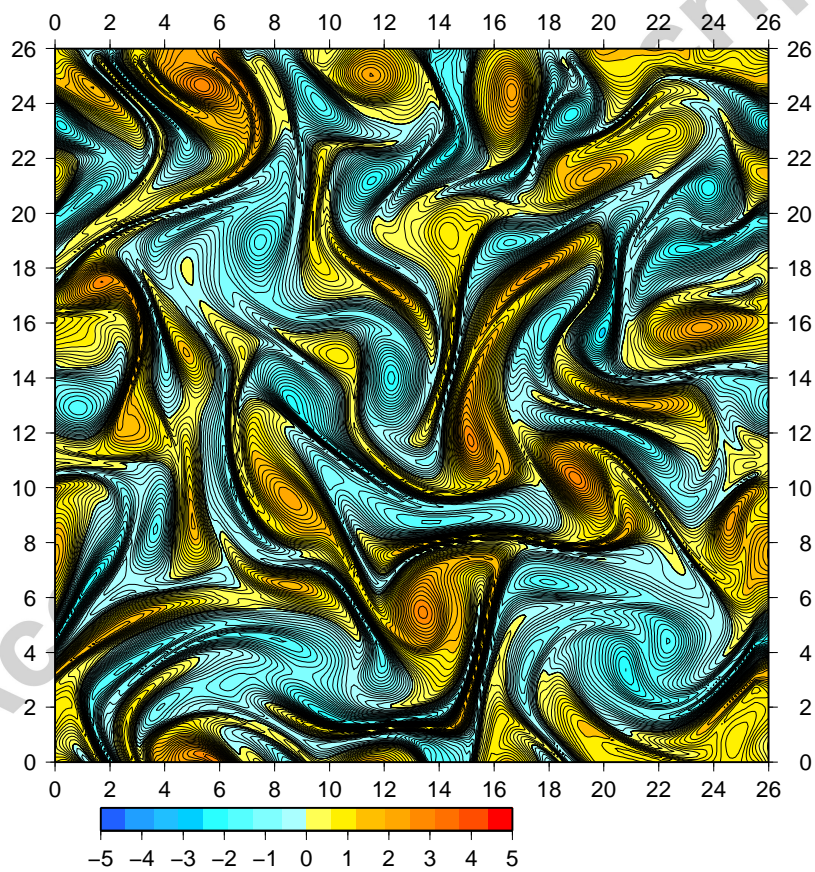


Figure 2: Snap shot of the vorticity field of the mean of the particle filter mean at time 50. Compare with figure 1 and note the close to perfect tracking.

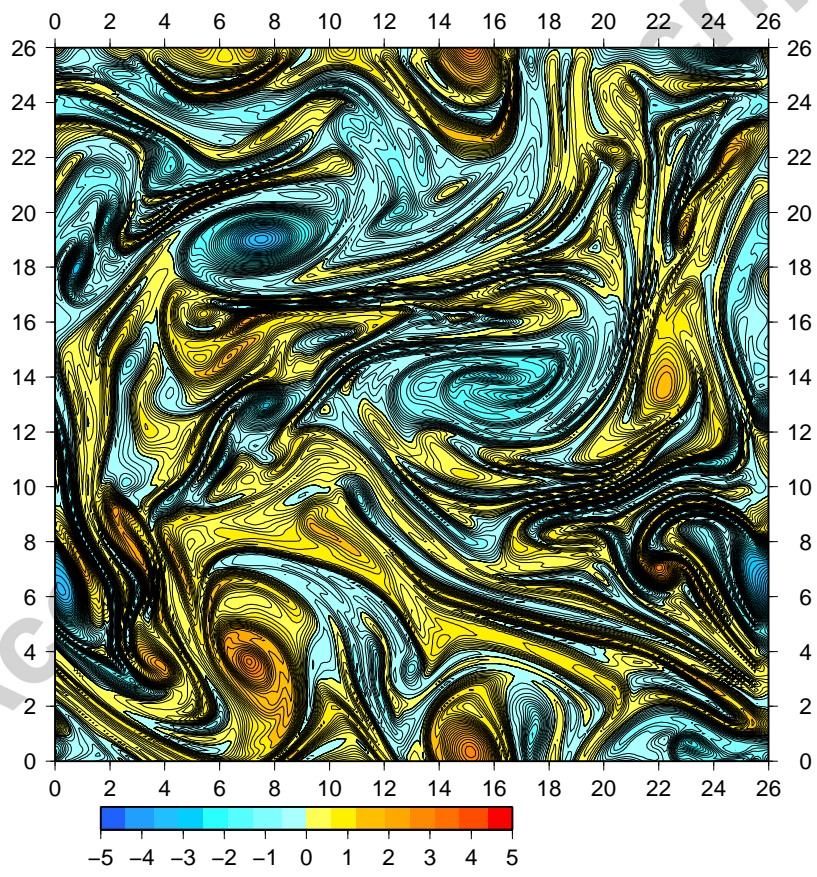


Figure 3: Snap shot of the vorticity field of the truth at time 600. Note again the highly chaotic state of the field.

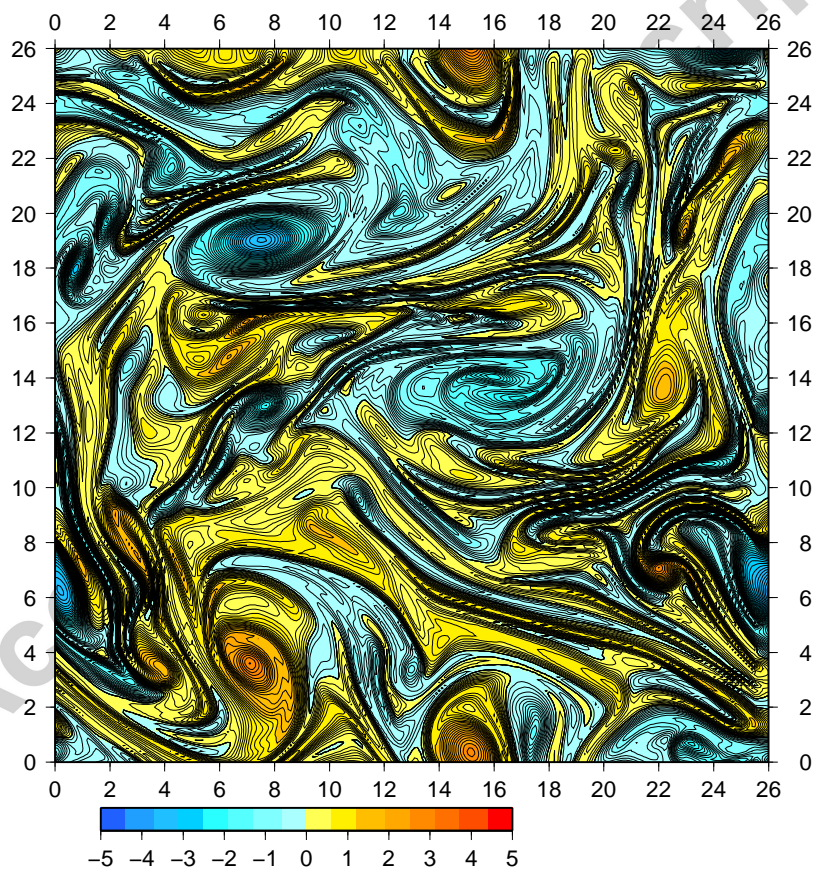


Figure 4: Snap shot of the vorticity field of the mean of the particle filter mean at time 600. Compare with figure 3 and note the close to perfect tracking.

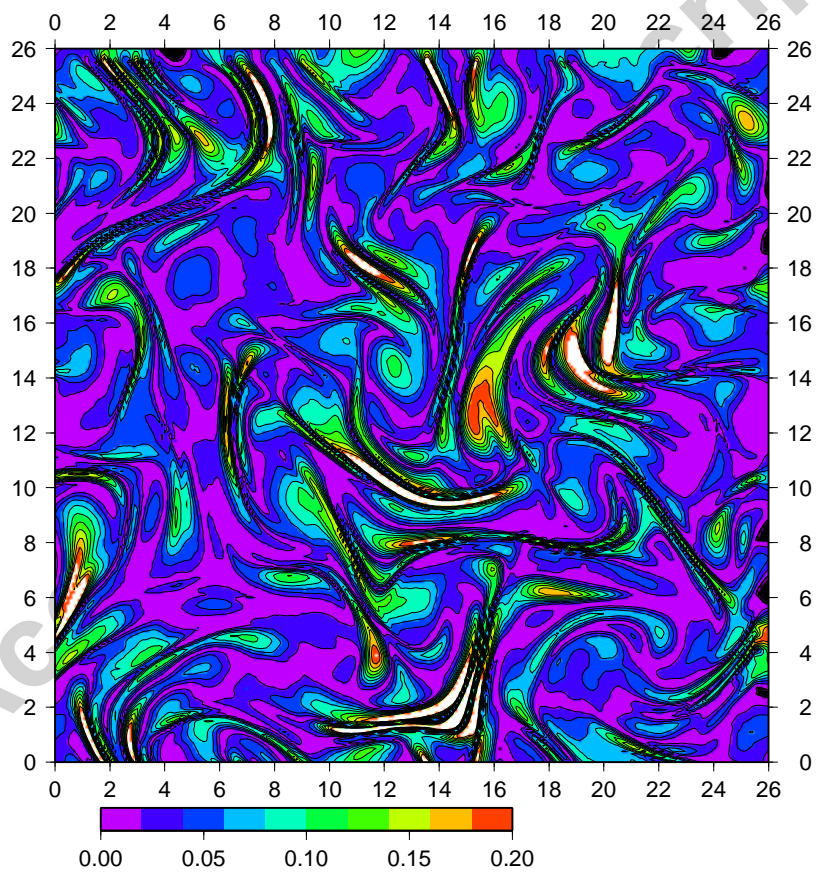


Figure 5: Snap shot of the absolute value of the mean-truth misfit at time 50. Note the highly irregularity of the field, reflecting the statistical nature of the estimate.

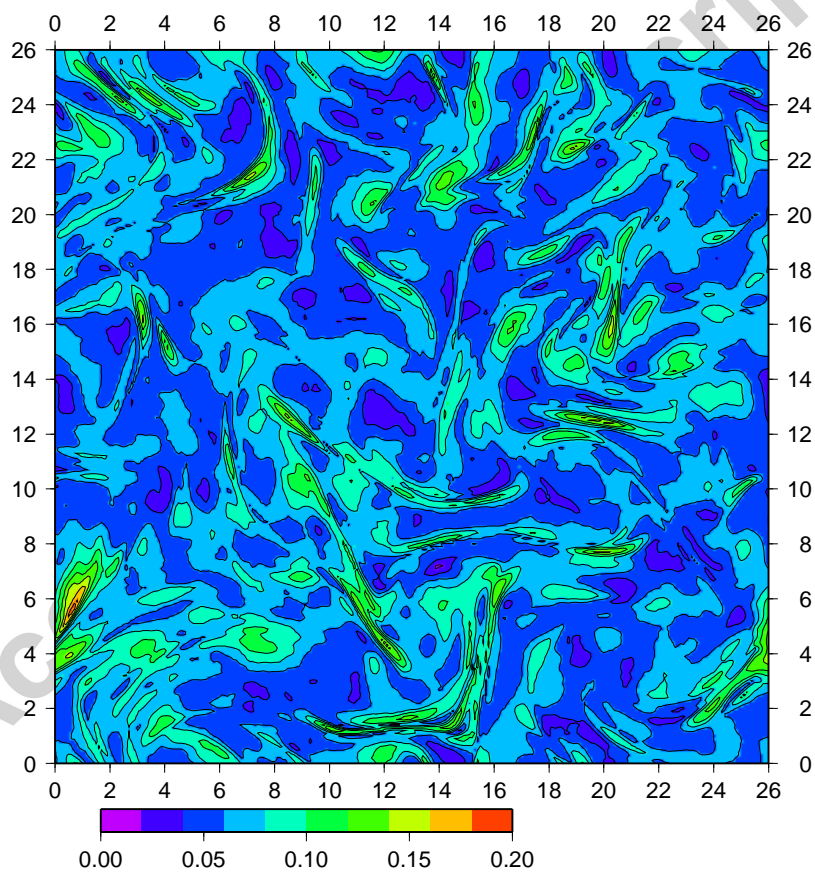


Figure 6: Snap shot of the absolute value of the standard deviation in the ensemble at time 50 for comparison with figure 5. The ensemble underestimates the spread at several locations, but averaged over the field it is slightly higher, 0.074 versus 0.056.

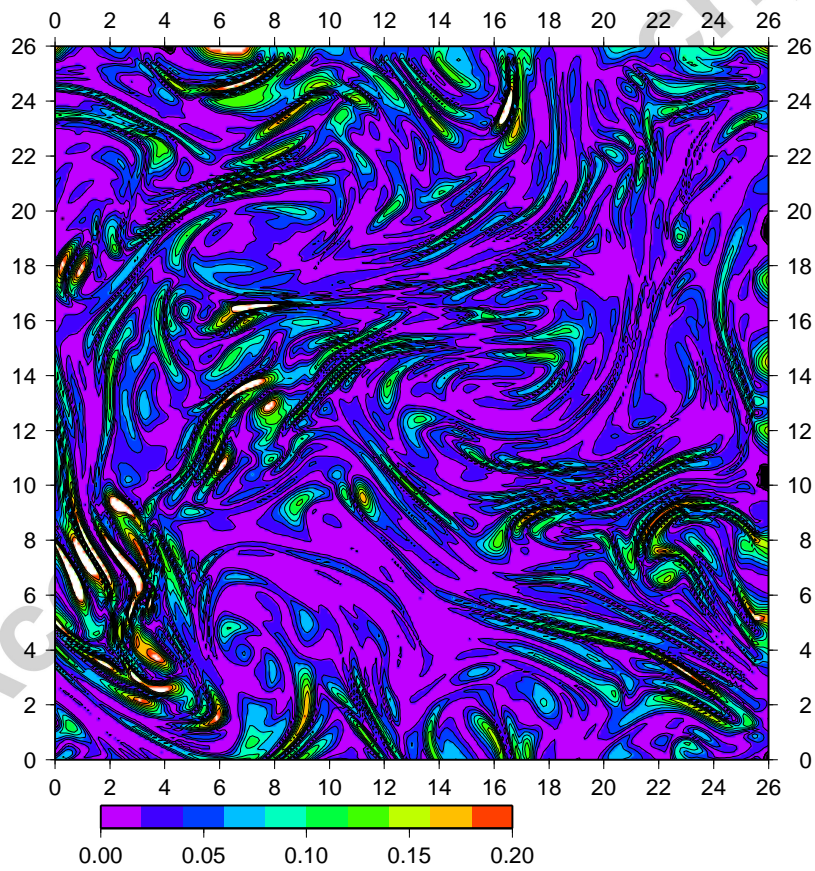


Figure 7: Snap shot of the absolute value of the mean-truth misfit at time 600.

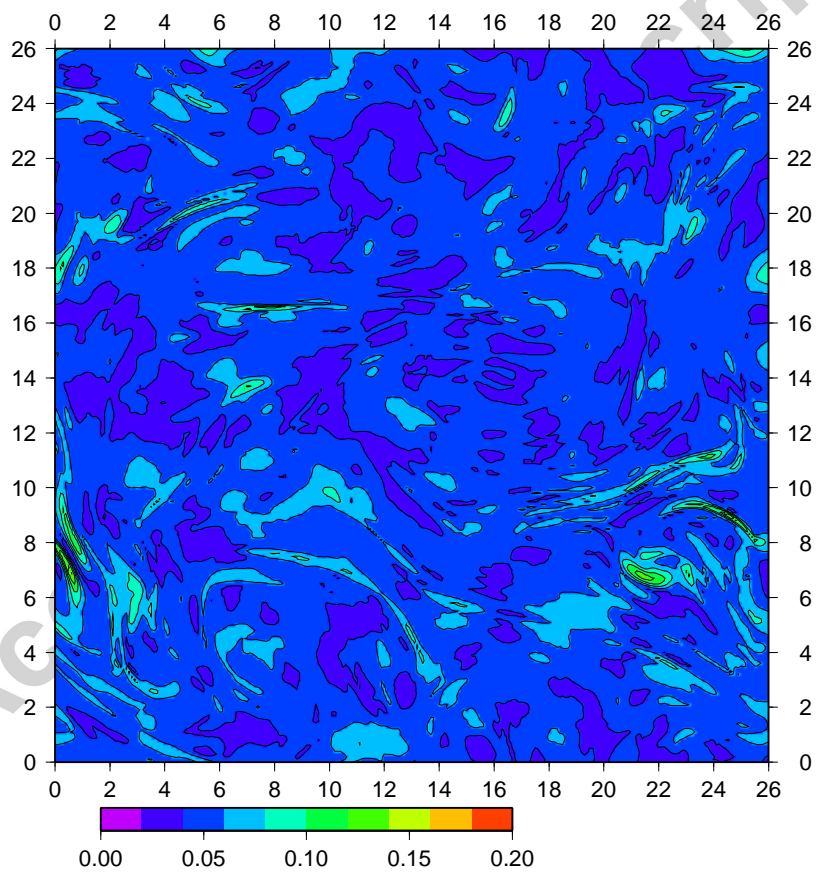


Figure 8: Snap shot of the absolute value of the standard deviation in the ensemble at time 600 for comparison with figure 7

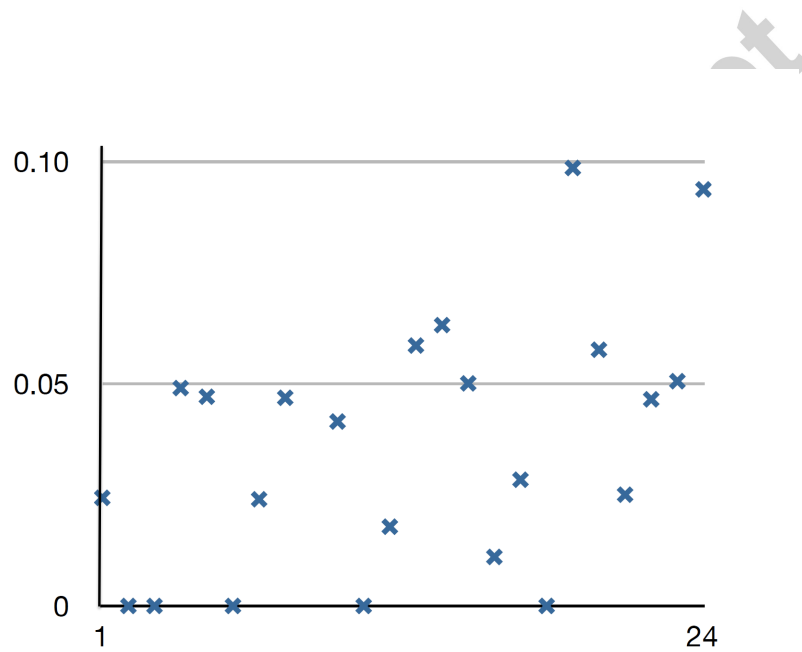


Figure 9: Weights distribution of the particles before resampling. All weights cluster around 0.05, which is close to $1/24$ for uniform weights (using 24 particles). The 5 particles with weights zero will be resampled. Note that the other particles form the smoother estimate.

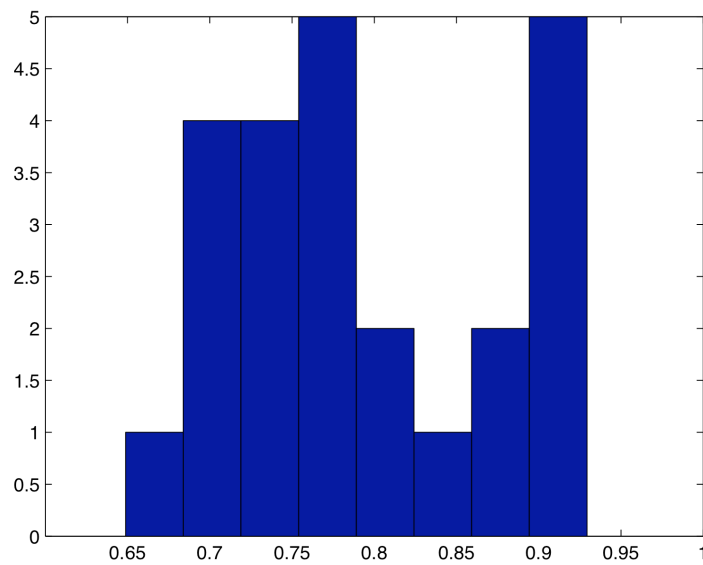


Figure 10: Estimate of the posterior pdf of the vorticity value at point (200,200) after 600 time steps. The bimodal structure shows that variational methods that look for the mode of this pdf have little meaning, and also methods based on the EnKF will not be able to represent this structure accurately.

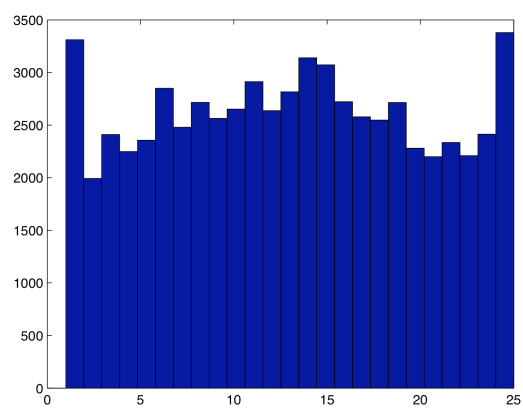


Figure 11: Rank histogram of how the truth ranks in the ensemble. The nearly uniform distribution shows that each particle could act as the truth, suggesting the ensemble is of good quality. (But see discussion in text.)

5 January 2012

Highlights:

1. First application of fully nonlinear data assimilation method to complex geophysical fluid dynamical system.
2. First application of full particle filter to 65,000 dimensional system
3. Detailed discussion of advantages and disadvantages of the new method